Highlights

Information Transmission and Processing in G-Protein-Coupled-Receptor Complexes

Roger D. Jones [a,b,c,e], Achille Giacometti[b,c], Alan M. Jones[a,d]

- A first-principles theory of molecular switches, validated by experiment, is presented.
- The model predicts three switch configurations: on, off, and intermediate.
- Switch state is controlled by free energy difference and externally driven chemical flux.
- Targeting dephosphorylation rates offers a potential drug strategy for switch modulation.

Information Transmission and Processing in G-Protein-Coupled-Receptor Complexes

Roger D. Jones [a,b,c,e], Achille Giacometti[b,c], Alan M. Jones[a,d]

[a]*Department of Biology University of North Carolina at Chapel Hill Chapel Hill North Carolina 27514 USA*
[b]*Dipartimento di Scienze Molecolari e Nanosistemi Universit"'a Ca' Foscari Venezia 30123 Venezia Italy*
[c]*European Centre for Living Technology (ECLT) Ca' Bottacin 3911 Dorsoduro Calle Crosera 30123 Venezia Italy*
[d]*Department of Pharmacology University of North Carolina at Chapel Hill Chapel Hill North Carolina 27514 USA*
[e]*Corresponding author: RogerDJonesPhD@gmail.com*

Abstract

We present a general theoretical framework for molecular computation in biological systems and apply it to G-protein-coupled receptors (GPCRs), which serve as central regulators of cellular information processing. Despite their importance, the physical principles underlying GPCR switching remain incompletely understood. Using nonequilibrium thermodynamics, we construct a model that accounts for GPCR switching observed in light-controlled, label-free impedance assays and identifies the parameters governing receptor-state transitions.

The framework shows that switching is governed by two factors: the ATP/GTP-driven chemical flux through the receptor complex and the free-energy difference between competing switch states. Together, these quantities determine the configuration of the switch. The model predicts that GPCRs can occupy three quasistable configurations, corresponding to "on," "off," and an intermediate state, each representing a local maximum in information transmission. Active states support sustained chemical flux, whereas inactive states do not.

The model incorporates two ligand-derived inputs: fixed structural features and inducible conformations such as *cis* and *trans* isomers. t further predicts that phosphatase activity, represented as an effective energy barrier, primarily determines whether the switch occupies the "on" or "off" state,

whereas kinase activity maintains flux without directly setting state occupancy. Comparison with label-free impedance measurements supports the existence of multiple quasistable states that depend on ligand conformation.

Because the framework relies on general nonequilibrium principles rather than system-specific biochemistry, it extends naturally to other biological switching systems driven by chemical flux.

Keywords:
G Protein-Coupled Receptor (GPCR), information flow, entropy, Second Law of Thermodynamics, phosphatse, nonequilibrium steady state, induced fit

---

1. Introduction

Biological systems are extraordinarily complex, often exhibiting behaviors that emerge from multilayered interactions across scales. This intricacy has prompted suggestions that living systems may resist reduction to a compact set of universal principles suitable for traditional mathematical modeling [18]. This raises the question of whether unifying theoretical principles might still be identified that help organize biological complexity beyond established frameworks such as cell theory [60], natural selection [47], and the enhanced Central Dogma [24]. Emerging theoretical perspectives, such as homeostasis [4], thermodynamics [43], information theory [3], and complexity theory [25], offer potential candidates for such organizing principles.

The aim of this study is to integrate key elements from these theoretical traditions to identify fundamental organizing principles of molecular computation with both scientific and practical relevance. We focus specifically on principles governing computation by G protein–coupled receptors (GPCRs), a class of proteins central to precision medicine and targeted therapeutics [70].

Biological systems can be interpreted as computational networks in which coupled chemical reactions act as molecular switches. Through these networks, cells process and transmit information that enables adaptive responses to changing environments. In contrast to neural computation, which is largely electrical, molecular information processing relies chiefly on membrane-associated chemical reactions distributed across tissues, with immune signaling providing a clear example.

Perturbations in these molecular information networks frequently contribute to disease, and many therapeutic strategies seek to restore or modulate their function. The rise of precision medicine [37, 39, 22] further emphasizes the need for pharmacological strategies that modulate molecular networks in a controlled and targeted manner to maximize therapeutic benefit while reducing adverse effects.

GPCRs represent a prominent class of molecular information processors, regulating cellular responses to external cues and enabling physiological adaptation across diverse environments [52, 42]. Through dynamic coupling to cytoplasmic partners such as G proteins and β-arrestins, GPCRs orchestrate a broad range of biological functions [41, 17]. A single GPCR may nonetheless generate contrasting physiological outcomes. Opioid receptors illustrate this duality: G-protein coupling mediates analgesia, whereas β-arrestin engagement contributes to tolerance and addiction [36, 38, 15]. These divergent outcomes underscore the challenge of selectively modulating GPCR signaling to maximize therapeutic efficacy while limiting adverse effects.

As in engineered computation, biological information processing requires continuous energy input and heat dissipation. GPCR signaling operates far from thermodynamic equilibrium, sustained by nucleotide hydrolysis (GTP $\rightarrow$ GDP) in G-protein switches and phosphorylation–dephosphorylation cycles (ATP $\rightarrow$ ADP) cycles [6] on the intracellular side of the receptor. Without these chemical fluxes, GPCR systems would relax to equilibrium, a state incompatible with sustained biological function. From an evolutionary perspective, and in line with nonequilibrium thermodynamics and information theory, molecular computation appears shaped by selective pressures that favor efficient energy use and high information throughput [49, 33, 67].

Mechanistic insight into these processes requires time-resolved assays that probe stimulus–response dynamics within GPCR complexes. Earlier studies largely characterized steady-state input–output relationships [14, 44], whereas Wirth et al. [68] advanced the field by using photoisomerizable ligands to modulate GPCR conformation in real time and by monitoring receptor activity via membrane impedance.

Building on these advances, we extend previous theoretical work [31, 32, 30] to interpret the resulting dynamic measurements. Our model identifies two fundamental parameters governing GPCR switching: the chemical flux through phosphorylation or GTPase cycles and the free-energy difference between the phosphorylated and dephosphorylated states. Both parameters

are influenced by ligand concentration and by ligand conformations that are either fixed or inducible.

The analysis shows that the switch can occupy three distinct configurations; on, off, and intermediate; rather than the conventional two states of engineered switches. Determining the switch state within this framework requires more than a single bit of information from the ligand, encoded in both its fixed chemical structure and in its inducible conformations. Fixed structures remain constant upon receptor binding, whereas inducible structures shift in response to external stimuli, such as light or conformational strain, arising from ligand–receptor interactions.

Experimental results support this interpretation: *cis* (Z) and *trans* (E) photoisomers of ligands modulate transitions not only between "on" and "off" states but also between active (flux-generating) and inactive (low-flux) modes. These discrete switching behaviors arise from the finite chemical flux that sustains the system.

Our model thus identifies two primary control inputs: the chemical flux within the switch and the binding energy associated with γ-phosphate groups (or equivalent nucleotides in G-protein systems). Mapping GPCR conformations within this control space offers a framework for the targeted modulation of molecular switches, a foundational step toward precise therapeutic control. A central open question concerns how the properties of the ligand influence these two control parameters.

2. Methods

2.1. Schematic of the Experiment

Conceptual schematic of the experimental setup from Wirth et al. [68] is shown in Figure 1. Chinese hamster ovary cells (CHO) were genetically engineered to overexpress the receptor, a member of the neuropeptide Y family, and cultured to confluence on a gold foil substrate [9]. This uniform expression of the receptor enabled for consistent detection of ligand-induced conformational changes via electronic impedance measurements across the gold foil.

Two wavelength-driven ligand isomers, cis (Z) and trans (E), were derived from azobenzene (ligand 28) and arylazopyrazole (ligand 30), producing four distinct GPCR inputs: E-28, Z-28, E-30, and Z-30. Z isomers were generated by 340 nm irradiation, while E-isomers were produced using 455 nm (ligand

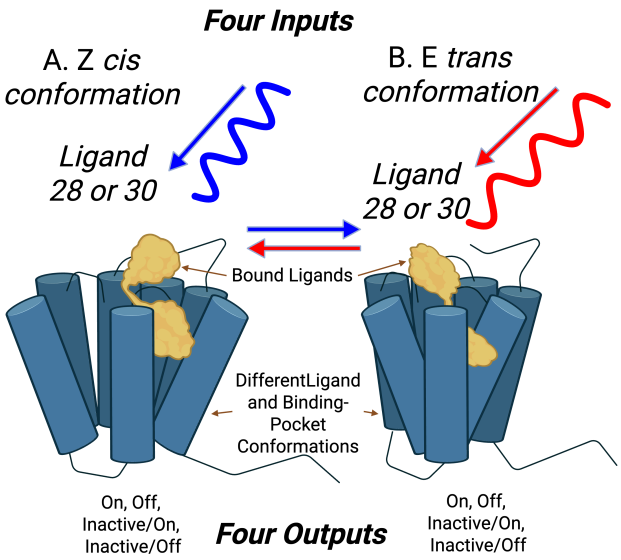

Figure 1: **Conceptual schematic of the experiment.** Ligands in cis (Z) or trans (E) configurations bind to GPCRs, while electrical impedance across a cell layer monitors signaling activity. Two engineered ligands (28 and 30) reversibly switch between Z and E isomers under wavelength-specific light (blue: Z→E; red: E→Z). Each conformation induces a distinct GPCR state, yielding four input combinations—encoding up to two bits of information. Experimental outputs map to four theoretical states: Active/On, Active/Off, Inactive/On, and Inactive/Off. However, impedance measurements cannot distinguish Inactive/On from Inactive/Off, so these are treated as a single 'Inactive' state. Theoretical modeling differentiates Active (flux-generating, dissipative) from Inactive (flux-free, non-dissipative) states

28) and 528 nm (ligand 30) light. GPCR response was inferred from changes in cell morphology, monitored by impedance measurements [61, 62, 66].

Natural downstream responses to activation of the Y_4 NPY receptor include reduced cAMP levels, context-dependent activation of PLC, and engagement of MAPK signaling pathways. The impedance measurement can also be viewed as a downstream, label-free response. In this interpretation, the switch behaves as a single conglomerate system that reflects the combined activity of the GTPase switch in the G protein and the phosphorylation–dephosphorylation cycles that generate the barcode.

No published data currently demonstrate that the specific receptor studied, when bound to the azobenzene- or arylazopyrazole-based ligands used in the Wirth experiments, activates a G protein and subsequently undergoes phosphorylation. Nevertheless, several recent studies have established that photoswitchable ligands can modulate GPCR activity in other systems. For example, Agnetta et al. showed that an azobenzene-containing dualsteric ligand can reversibly alter receptor efficacy upon light stimulation [1]. More recently, Duran-Corbera et al. demonstrated robust and reversible optical control of a native class A GPCR, the β_1 -adrenoceptor, using the photoswitchable ligand pAzo-2; light-induced *cis–trans* isomerization produced measurable changes in receptor activation in functional assays [13]. These studies collectively support the broader plausibility of using photoswitchable ligands to modulate GPCR signaling, even though direct evidence for the full sequence of events, ligand binding, G-protein activation, and phosphorylation, has not yet been reported for NPY with the specific ligands used here. Moreover, impedance measurements are a valid and measurable downstream response, even if not directly pharmacologically relevant. This is well demonstrated by Wirth et.al. [68].

2.2. Schematic of the Theory

To regulate cellular responses to external stimuli, biological information-processing systems must operate persistently and far from equilibrium, placing them in non-equilibrium steady states (NESS), a dynamic form of homeostasis. These states are maintained by continuous energy flow [e.g. ATP, GTP] from nucleotide hydrolysis and phosphorylation, with the entropy dissipated into the thermal bath.

The information content of an NESS remains stable over time, suggesting that it corresponds to a local or global extremum in information transmission. This aligns with the hypothesis that natural selection favors systems that maximize information flow under physical constraints. To formalize this, we quantify the information using mutual information [59] and apply the calculus of variations to identify the extrema, constrained by the constant chemical flux supplied by the input of nucleotide-driven energy.

2.3. Application to G Protein-Coupled Receptor Complexes

To demonstrate and validate the proposed theoretical framework, we focus on the fundamental process of information processing on the cell membrane. Among such processes, signaling through GPCRs plays a central role,

representing one of the most critical mechanisms in both biological regulation and medical intervention.

The foundation of the current GPCR model is illustrated in Figure 2, which schematizes the GPCR complex. In Figure 2A, the 7-transmembrane GPCR (blue) spans the membrane, interacting with both extracellular ligands (orange) and intracellular G proteins (purple, green, violet).

Ligand binding induces a conformational change in the GPCR, which enhances its affinity for heterotrimeric G proteins. This results in the formation of a ternary complex, comprising the ligand, GPCR, and G protein - that is more stable than the ligand receptor complex alone.[45].

The G protein α subunit (G_α) initially binds to GDP, representing the off state of the GTPase switch [52]. Upon GPCR activation, GDP is released and replaced by GTP, whose cellular concentration is maintained far from equilibrium. This GTP binding activates G_α, which completes the switch to the "on" state. The energy driving this transition derives from the thermodynamic disequilibrium between GDP and GTP.

The C-terminal tail of GPCR and the intracellular loops contain serine and threonine amino acid sites that can be phosphorylated/dephosphorylated by specific kinases/phosphatases. The C-terminal tail of GPCR and the intracellular loops contain serine and threonine amino acid sites that can be phosphorylated/dephosphorylated by specific kinases/phosphatases. The phosphorylation and dephosphorylation of these sites is known as a phosphorylation/dephosphorylation cycle (PdPC) that also acts as a molecular switch [52]. Similarly to the GTPase switch, the "on" and "off" states of these PdPC switches are determined by the phosphorylation status of specific sites. However, in this case, the switches are powered by the high concentration of adenosine triphosphate (ATP), which drives the process [5].

The collection of these PdPCs establishes a distinct molecular pattern, called a barcode, which serves as a guide for downstream signaling processes [69, 11]. Adapters read this phosphorylation barcode to propagate a certain response (Figure 2). In animals, this adapter is called β-arrestin [41] and in plants it is called VPS26A/B [29].

Furthermore, the flexible protein matrix surrounding the GPCR complex provides a mechanism to adjust energy levels and transition probabilities, facilitating changes in the conformation and behavior of the complex.

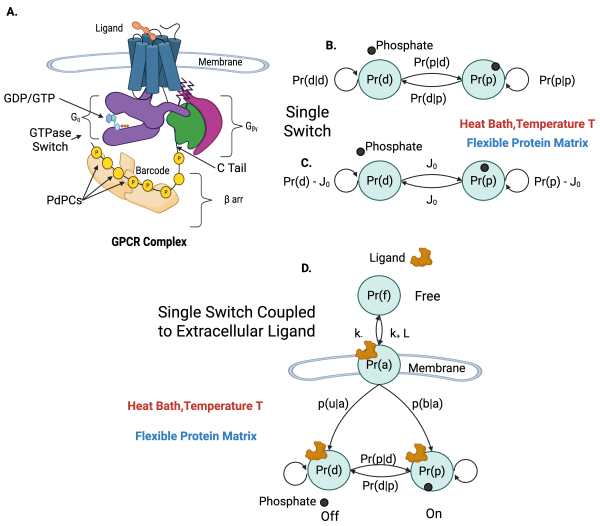

Figure 2: **Simple Molecular Switch A.** The 7-transmembrane GPCR is illustrated with blue cylinders representing the seven α helices that span the cell membrane. The extracellular ligand (orange) binds to the binding site of the GPCR inducing movement with the α helical bundles. The helices alter the conformation of the intracellular loops (thin black lines) of the GPCR complex. The intracellular portion of the complex has been separated for visibility. Two pathways may be activated, the G_α pathway (purple) and the βarr pathway (tan). The G_α subunit is a part of the G protein also composed of subunits β and γ. The βarr pathway is composed of additional response pathways determined by phosphorylation sites on the C tail of the GPCR and intracellular loops that form a barcode that encodes signals for downstream processes. **B.** Picture of a single switch taken to be a PdPC. A GTPase switch operates in the same manner. The switch resides in a heat bath at temperature T. In addition to the thermal bath, the switch is a component of a flexible protein complex that can modify energy barriers in the switch. Here, $\Pr(d)$ and $\Pr(p)$ are the probabilities of finding the receptor to be dephosphorylated and phosphorylated, respectively, while $\Pr(p|d)$ and $\Pr(d|p)$ are the conditional probabilities of finding the receptor has transitioned between phosphorylated to dephosphorylated positions and *vice versa*. **C.** Here, $J_0 = \Pr(p|d)\Pr(d) = \Pr(d|p)\Pr(p)$ is the steady-state probability flux among states. The flux is kept finite due to an external energy/entropy source. **D.** Three-state model: free receptor (f), phosphorylated (p), and dephosphorylated (d). The associated state a is bound to the ligand but not the phosphate. The associated state a has two internal states d and p. These two states form the G_α switch. Ligand dissociation and association reaction rates are given by k_- and k_+, respectively, and L is the ligand concentration. The picture for a GTPase switch is similar. A G protein-GDP is bound to $\Pr(a)$ and the ligand through a ternary reaction. The on state occurs when GDP is replaced with GTP.

3. Results

3.1. Experimental results relevant to this study

If the four input conditions produce four independent output responses, this corresponds to two bits ($\log_2 4$) of information transmitted across the membrane. Fewer distinct outputs would indicate reduced information transfer. If only the chemical structure of the ligand (for example, 28 versus 30) influences the response, then only one bit of information is transmitted. Observation of more than two outputs therefore implies that both the fixed chemical structure and the induced-fit conformations of the ligand [19] contribute to signaling.

The experiment reported in [68] revealed four distinct responses, demonstrating that both the Z and E photoisomerized conformations, along with the fixed structural differences between ligands 28 and 30, play essential roles in determining receptor output. This result indicates that each ligand can exist in two functionally distinct conformational states after light activation, enabling the full transmission of two bits of information through the receptor complex. These findings are consistent with independent observations of GTPase activity in other G proteins that display similar two-bit information transmission [35].

The ligand conformation was found to switch reversibly between *cis* and *trans* forms even while the ligand remained bound to the receptor. Importantly, removal of extracellular ligand did not alter the downstream response, which indicates that signaling is determined by the conformation of the bound ligand rather than by its continued presence in solution.

3.2. Theoretical Results

The theory developed here generalizes the widely used operational model of Black and Leff [8]. In the operational model, the switch state is governed by multiple applications of Michaelis–Menten kinetics [6], which produces a single solution for the output-state probability. In contrast, the framework presented in this study allows for up to three solutions, providing a richer and more flexible description of switch behavior.

The model described in Sections Appendix A.1, Appendix A.2 shows that a molecular switch can occupy quasistable states determined by two parameters: the chemical flux within the GPCR complex and the switch's free energy change. Both parameters are influenced by the extracellular

ligand's characteristics—its fixed and inducible conformations as well as its concentration outside the cell.

This framework leads to the Biological Ensemble, a generalization of the Canonical Ensemble from equilibrium statistical mechanics [53]. The Canonical Ensemble, described by Feynman as the "summit of statistical mechanics"[1] [16, Chapter 1], admits a single solution proportional to the exponential of the system energy [53]. In contrast, the Biological Ensemble introduced here yields three possible solutions that turns the ensemble into a system of switches, a key result of this work.

We illustrate the power of the Biological Ensemble with an intuitive analogy. Near thermochemical equilibrium, a system relaxes to a single state, much as air molecules uniformly fill a room at fixed temperature and density. In our framework, if those molecules were in an NESS, the room could instead exist in one of three distinct states: one resembling the usual equilibrium condition and two others in which all molecules cluster into two different corners of the room. In this analogy, the NESS behaves as a switch with three possible configurations. It is clear that a room in equilibrium and a room in NESS are fundamentally different, and each would exhibit markedly different behavior.

The solutions correspond to local maxima of information flow, quasi-stable states that can transition under perturbation. Two parameters govern which state the switch occupies: (1) the energies of the phosphorylated (E_p) and dephosphorylated (E_d) conformations, and (2) the chemical flux J_0 from the phosphorylation/dephosphorylation cycle. Together, these parameters determine whether the switch is in the "off", "on" or intermediate configuration.

The energy parameter is given by the normalized change in the Gibbs free energy going from the "off" to "on" switch configuration.

$$\beta(E_p - E_d) \tag{1}$$

where β is the inverse of the temperature of the heat bath (Boltzmann constant = 1). The Gibbs free energy is the valid form of free energy to use since

[1] "This fundamental law is the summit of statistical mechanics, and the entire subject is either the slide-down from this summit, as the principle is applied to various cases, or the climb-up to where the fundamental law is derived and the concepts of thermal equilibrium and temperature T clarified." R. P. Feynman

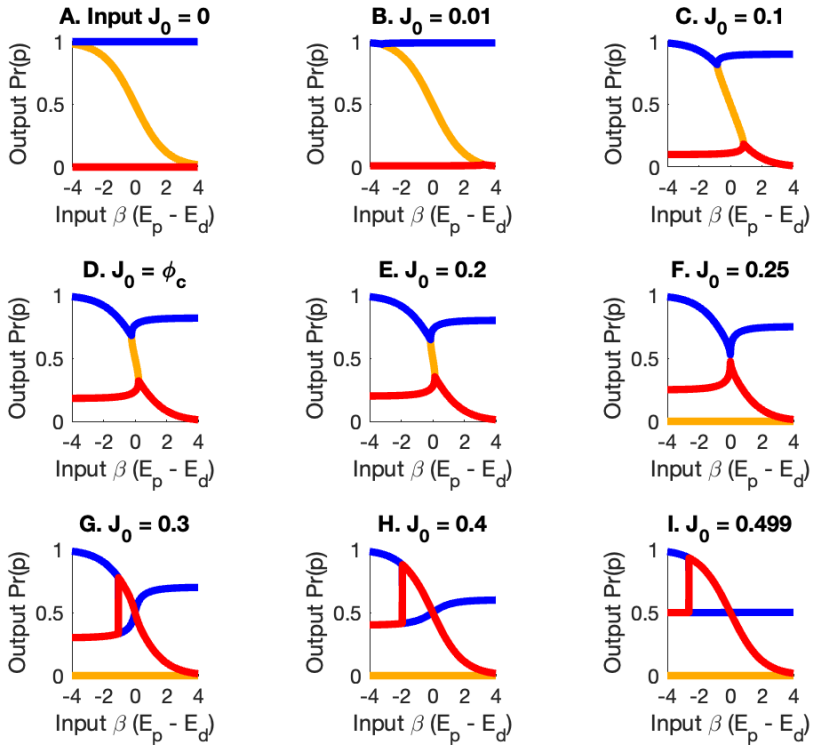

Figure 3: The three solutions for $\Pr(p)$ for the Biological Ensemble as a function of the chemical flux J_0 and change in free energy between two receptor states $\beta(E_p - E_d)$. **A.** In the limit of small flux, the solutions are (1) $\Pr(p) = 1$, $\Pr(d) = 1 - \Pr(p) = 0$ (blue), (2) $\Pr(d) = (1 - \Pr(p) = 1$, $\Pr(p) = 0$ (red), and (3) the Canonical Ensemble of (yellow). **B.-F.** For small values of flux J_0, The highest information path for probability $\Pr(p)$ obeys the Canonical Ensemble. The thermodynamic branch steepens as the chemical flux J_0 increases. **G.-I.** A discontinuity forms in the kinetic branch and the two solutions exchange roles with increasing change in free energy. For fluxes less that the critical flux $\phi_c \approx 0.182$

the system is in a heat bath at temperature $T = 1/\beta$ and no external work is being applied to the system. The energies E_p and E_d are modified from their baseline measured values ($\approx$ 7 kcal/mol) [54] by the presence of the protein matrix of the GPCR complex. Modifications as high as 17 kcal/mol have been seen in the muscles of athletes [65].

If R_p and R_d are the numbers of receptors in the phosphorylated ("on") and dephosphorylated ("off") switch configurations, then the probability of

the receptor being in each of the switch configurations is

$$\Pr(p) = \frac{R_p}{R_d + R_p} \tag{2}$$

and

$$\Pr(d) = 1 - \Pr(p) = \frac{R_d}{R_d + R_p} \tag{3}$$

for the phosphorylated and dephosphorylated configurations, respectively.

We define the chemical flux J_0 as the flow of probability from one switch configuration to the other.

$$J_0 = \Pr(d)\ \Pr(p|d) = \Pr(p)\ \Pr(d|p) \tag{4}$$

where $\Pr(p|d)$ is the probability that the receptor state transitions from configuration d to p and $\Pr(d|p)$ is the probability of transition in the opposite direction. The equality sign is a consequence of the steady-state requirement and is an expression of Bayes Theorem [23].

The terms in Equation 4 are intuitive from a chemist's perspective. The probability $\Pr(d)$ is proportional to the chemical concentration of the system in the dephosphorylated configuration, while $\Pr(p)$ is proportional to the concentration of the phosphorylated concentration. The transition probabilities $\Pr(p|d)$ and $\Pr(d|p)$ are the reaction rates.

An intuitive schematic of the information landscape is provided in Appendix C, illustrating how the system navigates between quasistable states. The figure represents a landscape in which the curves are ridges of maximum switch information. Three solutions exist for the probability $\Pr(p)$ that the switch is in the "on" configuration for each flux and change in free energy value. In the limit of small flux, the solutions are (1) $\Pr(p) = 1,\ \Pr(d) = 1 - \Pr(p) = 0$ (blue), (2) $\Pr(d) = 1 - \Pr(p) = 1,\ \Pr(p) = 0$ (red), and (3) the Canonical Ensemble (yellow). We define solution (3) as the thermodynamic branch, while solutions (1) and (2) are defined to be the kinetic branch.

For small values of flux J_0, the highest information path, the thermodynamic branch (yellow), for probability $\Pr(p)$ obeys the Canonical Ensemble. The thermodynamic branch steepens as the chemical flux J_0 increases. At $J_0 = \phi_c \approx 0.182$, the information content of the kinetic branch becomes equal to the information of the thermodynamic branch. For $J_c > \phi_c \approx 0.182$, the information in the kinetic branch is greater than the information in the Thermodynamic Branch. This implies that for flux greater than ϕ_c, the states in

the kinetic b ranch are more stable than the states in the thermodynamic branch. The opposite is true for $J_0 < \phi_c$.

At $J_0 = 1/4$, the thermodynamic branch is given by $\Pr(p) = 0$. For $J_0 > 1/4$, a discontinuity forms in the kinetic branch and the two solutions exchange roles as the change in free energy increases.

The curves in Figure 3 represent local maxima of information transmission, corresponding to quasi-stable states defined by chemical flux J_0 and change in free energy $\beta(E_p - E_d)$. Here β is the inverse temperature of the heat bath, E_p is the energy of the phosphorylated "on" state and E_d is the energy of the dephosphorylated "off" state. These configurations act as local attractors, indicating preferred switch states within the control space.

Observed switch behavior is expected to align with these quasi-stable states. The Biological Ensemble framework shows how variations in J_0 and $\beta(E_p - E_d)$ guide the system into specific configurations, offering predictive insight into the switch dynamics under varying conditions.

A simple water-pump analogy, presented in the Discussion, offers a macroscopic visualization of the mechanism by which the switch transitions between these states.

3.3. Comparison of Theory and Experimental Results

The experimental results from Wirth et al. are depicted in Figures 4A and B, alongside the theoretical predictions. The mapping from impedance to probability is given in Appendix B. Solid and dashed red lines show impedance responses for ligands 28 and 30 initially prepared in the Z/on and Z/off configurations, respectively; blue lines represent E/on (solid) and E/off (dashed) preparations. The solid black line shows the response to the endogenous ligand hPP, and the dashed black line corresponds to the solvent control (DMSO). Figure 4A shows the results for ligand 28, and Figure 4B for ligand 30. Green lines indicate ligands prepared in the Z/on (dashed) and E/on (solid) states that were alternately irradiated with short (340 nm) and long (455 nm for 28; 528 nm for 30) wavelengths.

Figure 4C–F present schematic summaries of the experimental transitions among quasi-stable switch configurations. Figure 4C shows that for ligand 28 in the E/on configuration, the impedance remains similar to that of Z/on. The off" states (E/off and Z/off) also overlap. Initial 340 nm irradiation slightly increases impedance but does not shift the system out of E/on. Subsequent alternating irradiation causes the system to toggle between E/on and Z/off, indicating that cis (Z) favors the "on" state and trans (E) favors "off."

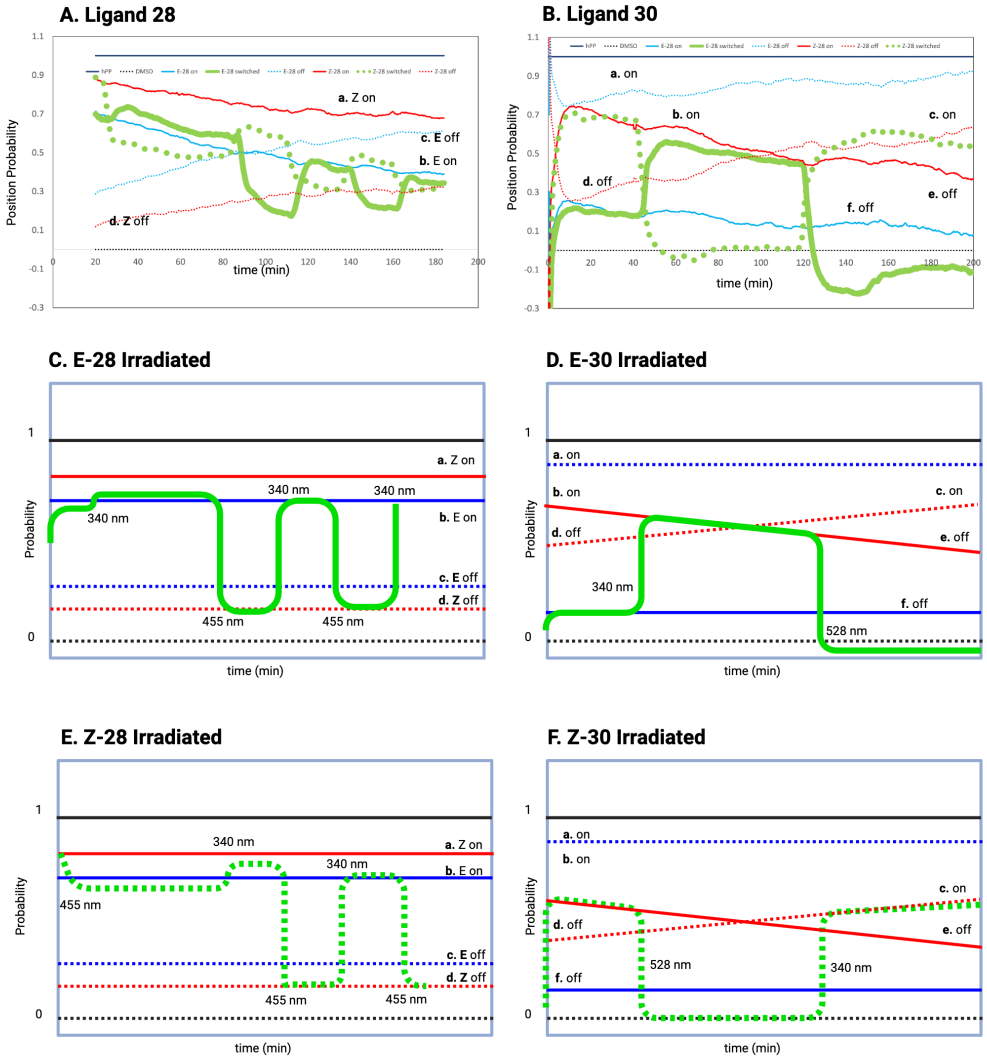

Figure 4: **A. and B.** Experimental Results **C.-F.** Schematic of Quasistable States. For Ligand 28, irradiation with wavelengths 340nm and 455 nm toggle the the system between the E/on (trans) and the Z/off (cis) states. For Ligand 30, irradiation with 340 nm and 528 nm toggles between active and inactive configurations.

Figure 4E shows the system initialized in the Z/on state. After a brief stable period, alternating light induces switching between Z/off and E/on,

again confirming the correlation between the cis/trans states and switching on/off for ligand 28.

For ligand 30 (Figures 4D and F), the Z/on and Z/off responses overlap, indicating that the "on"/"off" distinction does not apply. Instead, the system transitions between an active Z state that supports chemical flux and an inactive E state that does not. Thus, ligand 30 modulates switch activity versus inactivity, rather than discrete "on"/"off" signaling. Ligand 28 toggles the switch between on and off based on Z/E conformation, while ligand 30 toggles between active and inactive states. These behaviors reflect different modes of ligand control over GPCR switching.

The mapping of the experimental observations onto the theoretical framework is shown in Fig. 5, which enlarges the regions highlighted in Figs. C.8E and A. The theory assumes that the system preferentially occupies active portions of the solution curves that support high information flow, indicated in black. The inactive state, corresponding to zero phosphorylation, appears as a dashed red curve. Ligand 28 alternates between active on and active off states depending on its conformation, whereas ligand 30 toggles between an active on state and an inactive off state.

In Fig. 5, the flux was set to $J_0 = 0.2$, ensuring that the energy $\beta(E_p - E_d)$ at the transition points is approximately one. This balance is essential for both stability and switching efficiency. When $\beta(E_p - E_d)$ is much less than one, thermal fluctuations destabilize the quasistable states. When it is much greater than one, the states become so stable that switching is no longer feasible, preventing computation. This tradeoff was already recognized by Schrödinger in early discussions of biological information flow [58, 50]. The Wirth experiment therefore implies that the flux J_0 and the energy $\beta(E_p - E_d)$ fall near 0.2 and 1, respectively, illustrating how these otherwise inaccessible parameters can be inferred indirectly from experimental assays.

4. Discussion

Biological switches operate far from thermochemical equilibrium and rely on continuous entropy flow sustained by external chemical fluxes. As a result, equilibrium thermodynamics cannot adequately describe molecular information processing. The functional states of molecular switches correspond to homeostatic nonequilibrium steady states that persist within the ongoing entropy flow characteristic of living systems. The thermodynamics of these

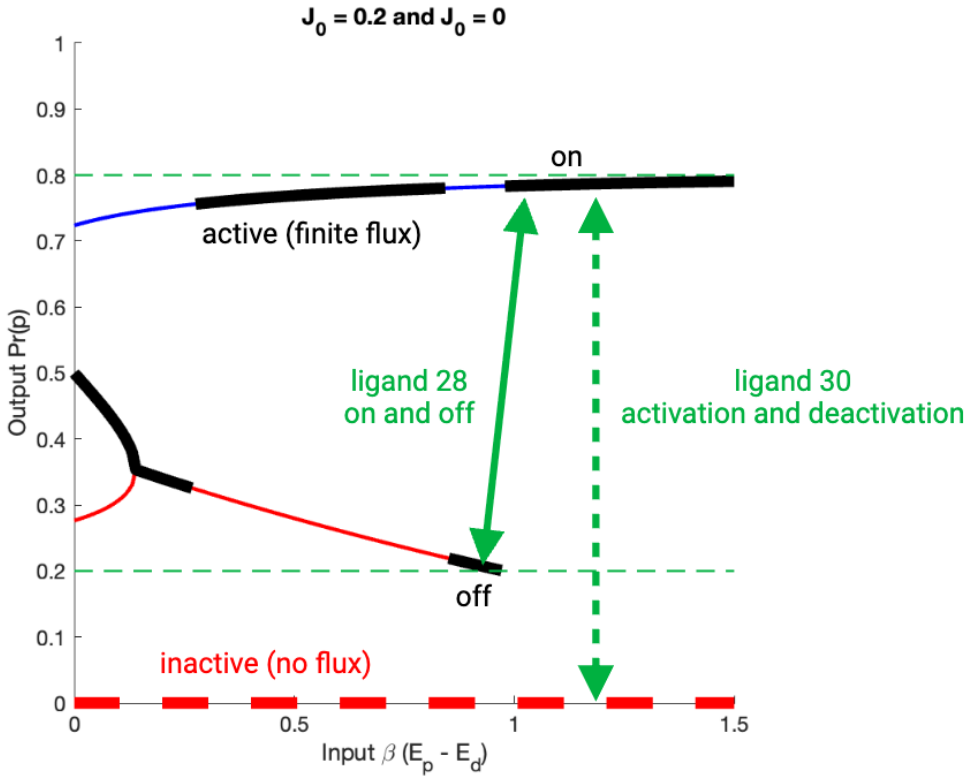

Figure 5: Blowup of Figures C.8E and A from the Appendix. According to the assumptions in the theory, the system favors states with higher information flow, which are outlined in black. The solid blue and red curves are the active on and active off states of the switch for $J_0 = 0.2$. The dashed red curve is the off state for an inactive switch ($J_0 = 0$). The theory predicts that ligand 28 in the Wirth experiment toggles between on and off states, depending on the ligand conformation, while ligand 30 toggles between the active on state and the inactive state of the switch. Ligand 28 can be toggled by small adjustments in the energy $\beta(E_p - E_d)$, while ligand 30 can be toggled by adjusting the flux J_0 between 0 and 0.2. The energy $\beta(E_p - E_d)$ needs to be approximately equal to one in order to balance switch stability with the ability to toggle switch states efficiently. The flux must lie between approximately 0.2 and approximately 0.3 in order to observe distinct on and off states and to maintain the energy $\beta(E_p - E_d)$ approximately equal to one (See Figure C.8).

states differ fundamentally from equilibrium descriptions that emphasize free-energy minimization. Instead, sustained energy and entropy flux give rise to

switching behavior that is richer than the dynamics available at equilibrium.

The strength of the thermodynamic approach lies in its ability to isolate the essential features of a system and filter out unnecessary detail. For example, marbles placed in a bowl always settle at the bottom regardless of their size, mass, friction, or path taken. If the goal is to identify the final state, thermodynamics is sufficient. Understanding complex biological systems likewise requires attention to coarse-grained, functionally essential features rather than detailed molecular mechanisms. Natural selection favors systems that perform their required functions, much as engineers design steam engines suited to specific tasks. Engines optimized for flat terrain differ from those designed for steep inclines, and studying only one context does not reveal the general principles that govern all engines.

The same logic applies to conserved biological processes. Although molecular details vary across species, the core functional architecture is preserved. Focusing exclusively on specific instances can obscure these general principles. An alternative strategy is to assume that a system optimizes a particular quantity, such as efficiency or information transmission, and infer the system features that maximize it. Here, we adopt this principle-based strategy to explore molecular switches that maximize information processing. This framework produces predictions consistent with experimental data and provides a unified view of molecular signaling dynamics.

For GPCRs, the flux J_0 represents transitions among intermediate, off, and on configurations. These advanced biological information-processing units erase information and thereby generate heat and entropy [40], which underscores the thermodynamic requirement for chemical flux. Without flux, biological computation cannot proceed. To capture this behavior, we introduce the Biological Ensemble, which extends classical free-energy minimization to include chemical flux and information flow. The formulation in Appendix A.1 enables prediction of switching dynamics outside the scope of equilibrium theory.

A conceptual analogy is provided in Figure 6. A pump drives water between two buckets that represent the on and off receptor states, while water height reflects state probability. The pump, analogous to an ATP or GTP driven kinase, maintains chemical flux. The energy barrier, represented by the return tube height, models phosphatase activity that regulates resistance to reverse flow. Heat generated by the pump dissipates into the surrounding environment. In this analogy, the phosphatase determines relative occupancy of the on and off states, whereas the kinase maintains flux.

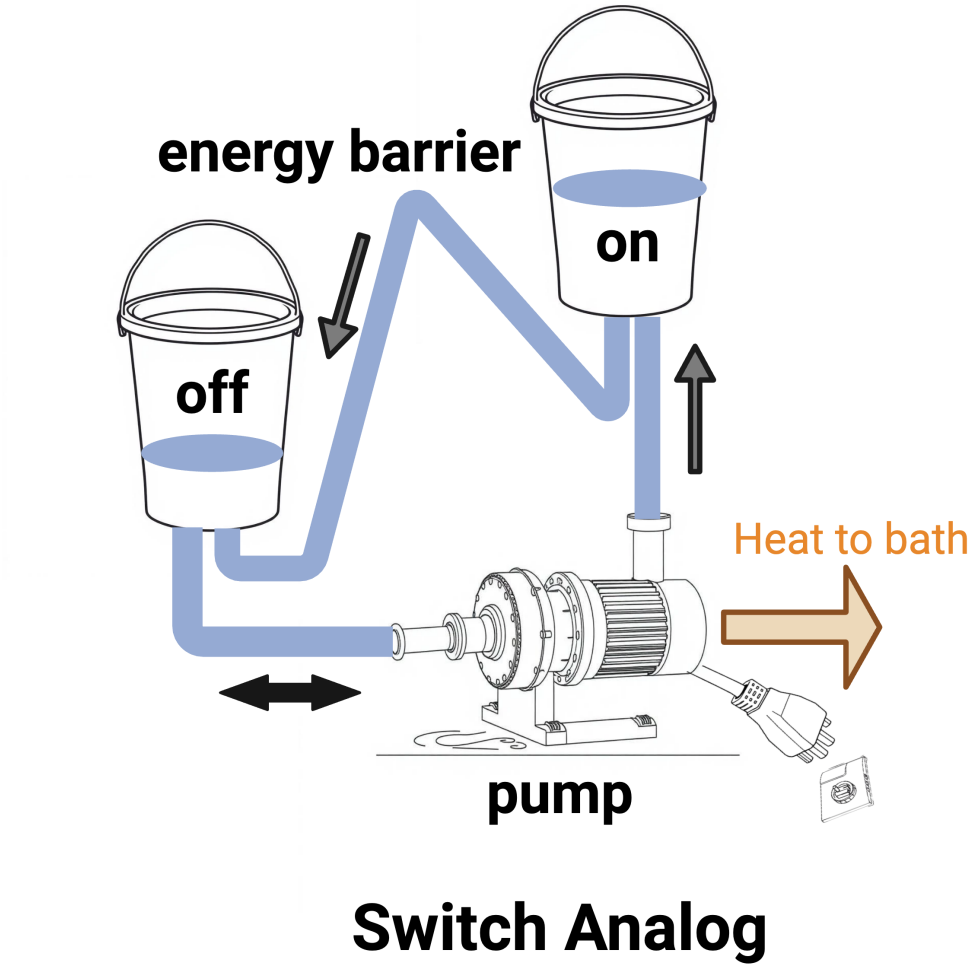

Figure 6: The "on" and "off" switch conformations are modeled as water buckets labeled on and off, where water levels represent the probability of each receptor state. Forward flow fills the on bucket, while reverse flow fills the off bucket. A pump, analogous to ATP/GTP-driven energy input, powers the cycle. The flow magnitude and state occupancy are regulated by an energy barrier, represented by the height of the return tube, which controls resistance to reverse flow.

The model identifies two behavioral regimes. At low flux J_0, the system operates near equilibrium and is dominated by thermal effects. As J_0 increases, the dynamics shift to a kinetic branch governed by nonlinear effects. The equilibrium solution, shown as the yellow curve in Figure 3A, repre-

sents the global maximum of information flow. Additional nonequilibrium steady states, shown in red and blue, represent local maxima that do not appear in equilibrium treatments. As J_0 grows, these nonequilibrium solutions diverge from equilibrium predictions. At a critical flux value, the kinetic branch exceeds the thermodynamic branch in information content, marking a qualitative shift in system behavior.

The free-energy difference $\beta(E_p - E_d)$ and the flux J_0 are subject to upstream regulation. Ligand-induced conformational changes primarily modulate $\beta(E_p - E_d)$, while J_0 depends on ligand concentration and binding. Without ligand, flux cannot be maintained. Ligand structure and availability therefore function as higher-order regulators of switch behavior [31, 32]. Classical biochemical approaches that rely on free-energy minimization alone are insufficient for systems requiring continuous energy and entropy input.

Although $\beta(E_p - E_d)$ and J_0 are difficult to measure directly, they can be inferred from assay data, including impedance measurements such as those of Wirth et al. [68]. Early work in information maximization and maximum entropy production provided precursor methods for these inferences [31, 32]. Transitions among the intermediate, off, and on states correspond to transitions among quasistable states in the information landscape of Figures 3 and C.7. These transitions are induced by allosteric conformational changes triggered by ligand binding, although the detailed mechanisms lie beyond the scope of this study. Once such transitions are identified experimentally, the corresponding values of $\beta(E_p - E_d)$ and J_0 can be inferred. Future work will extend this analysis to arrays of switches.

Applied to GPCR signaling, the framework explains how two ligand-derived bits of input, the chemically fixed identity of the ligand (28 or 30) and its inducible conformation (Z or E), produce four receptor output states: active on, active off, inactive on, and inactive off. Because the measurements were label-free, they did not distinguish between GTPase and PdPC based switching. This distinction is not critical here because the framework applies to both. Active states display significant flux and heat generation, whereas inactive states do not. On and off refer to phosphorylation or nucleotide binding. The presence of four distinct outputs indicates that the two, Z/E and 28/30, inputs are independent; correlated inputs would have produced fewer outputs. This suggests that photoisomerization generates complex conformational changes that encode information beyond simple geometric rearrangements. Ligand concentration also carries information [30].

Although we focused on phosphorylation and dephosphorylation as a

representative switch, the framework applies to any binary reaction-based switch. Nucleotide exchange reactions, central to GPCR signaling, obey the same fundamental thermodynamic principles [52]. Given GPCR coupling architecture, switching in the Wirth experiment likely reflects nucleotide-driven processes.

Biological switches operate in networks influenced by interactions with partner proteins, membrane environments, and covalent modifications such as lipidation and disulfide bonding. These features influence both free energy and flux. A strength of the thermodynamic approach is its predictive power without detailed mechanistic information. Just as a ball reaches the bottom of a bowl regardless of its precise trajectory, molecular switches reach their final nonequilibrium steady state regardless of microscopic details, provided the energy and flux constraints are known.

Although the present study does not address the phosphorylation barcode that governs β-arrestin signaling, future work will explore how ligand concentration and activation sequence encode additional information. Experimental response curves can test these predictions [30].

Finally, although this study focuses on GPCR-mediated signaling, the theoretical framework is broadly applicable. GPCRs account for roughly 30 percent of approved drugs [55], yet phosphorylation and nucleotide-exchange cycles function as universal molecular switches in many pathways. Similar architectures operate in receptor tyrosine kinases [57] and Toll-like receptors [10]. The principles developed here may therefore extend across a wide range of biological systems and offer a unifying thermodynamic basis for molecular information processing. Our results indicate that such generality is plausible, but additional experimental comparisons will be required to confirm this broader applicability.

5. Conclusions

1. A general theoretical framework for molecular computation in biological systems has been developed using nonequilibrium thermodynamics and information theory.
2. The theory predicts that biochemical switches, including GPCR complexes, can occupy up to three quasistable states—on, off, and an intermediate configuration, each associated with a local maximum in information transmission.
3. Two fundamental control parameters determine switch behavior:

- the nonequilibrium chemical flux generated by phosphorylation or GTPase cycles, and
- the free-energy difference between the phosphorylated and dephosphorylated states

4. Mapping the theory to light-controlled impedance assays from Wirth et al. [68] shows that the experimental responses are consistent with transitions among the predicted quasistable states.
5. The analysis suggests that phosphatase activity primarily sets on/off occupancy by controlling the effective energy barrier, while kinase activity sustains flux without directly selecting the switch configuration.
6. Because the framework relies on general nonequilibrium principles rather than GPCR-specific biochemistry, it has the potential to be broadly applied to other biological switching systems.

6. Acknowledgements

We thank Prof. Joachim Wegener and his team for generously providing the raw data used in our analysis. We also thank Katherine Newhall for valuable insights on macroscopic reversibility. Research by AG is supported by MIUR PRIN-COFIN2022 grant 2022JWAF7Y. The figures were generated with Blender. The cubic equations were solved with Mathematica. Numerical calculations were performed with MATLAB.

7. Author Contributions

RDJ: Conceptualization, Formal analysis, Investigation, Methodology, Project administration, Software, Writing – original draft. AMJ: Conceptualization, Investigation, Validation, Writing – review and editing. AG: Conceptualization, Formal analysis, Methodology, Writing – review and editing.

8. Funding

Research in the laboratory of AJ is supported by the National Science Foundation (MCB-0718202) and the National Institute of General Medical Sciences (R01GM065989).

9. Glossary

- ATP: Adenosine Triphosphate
- CHO: Chinese hamster ovary
- GPCR: G Protein Coupled Receptor
- GTP: Guanosine Triphosphate
- NESS: Nonequilibrium Steady State

References

[1] Agnetta, L., Kauk, M., Canizal, M.C.A., Messerer, R., Holzgrabe, U., Hoffmann, C., Decker, M.: A photoswitchable dualsteric ligand controlling receptor efficacy. Angewandte Chemie International Edition **56**(25), 7282–7287 (2017)

[2] Ash, R.B.: Information theory. Courier Corporation (2012)

[3] Bajić, D.: Information theory, living systems, and communication engineering. Entropy **26**(5), 430 (2024)

[4] Bechtel, W., Bich, L.: Situating homeostasis in organisms: maintaining organization through time. The Journal of Physiology **602**(22), 6003–6020 (2024)

[5] Berg, J.M., Tymoczko, J.L., Stryer, L., et al.: Biochemistry (2002)

[6] Berg Jeremy, M., Tymoczko John, L., Gatto Jr Gregory, J., Lubert, S.: Biochemistry. W. H. Freeman (2019)

[7] Bernadó, P., Mylonas, E., Petoukhov, M.V., Blackledge, M., Svergun, D.I.: Structural characterization of flexible proteins using small-angle x-ray scattering. Journal of the American Chemical Society **129**(17), 5656–5664 (2007)

[8] Black, J.W., Leff, P.: Operational models of pharmacological agonism. Proceedings of the Royal society of London. Series B. Biological sciences **220**(1219), 141–162 (1983)

[9] Cabrele, C., Beck-Sickinger, A.G.: Molecular characterization of the ligand–receptor interaction of the neuropeptide y family. Journal of peptide science: an official publication of the European Peptide Society **6**(3), 97–122 (2000)

[10] Chattopadhyay, S., Sen, G.C.: Tyrosine phosphorylation in toll-like receptor signaling. Cytokine & growth factor reviews **25**(5), 533–541 (2014)

[11] Chen, H., Zhang, S., Zhang, X., Liu, H.: Qr code model: a new possibility for gpcr phosphorylation recognition. Cell Communication and Signaling **20**(1), 1–16 (2022)

[12] Dönertaş, Ş.: Role of thought experiments in solving conceptual physics problems (2011)

[13] Duran-Corbera, A., Faria, M., Ma, Y., Prats, E., Dias, A., Catena, J., Martinez, K.L., Raldua, D., Llebaria, A., Rovira, X.: A photoswitchable ligand targeting the β1-adrenoceptor enables light-control of the cardiac rhythm. Angewandte Chemie International Edition **61**(30), e202203449 (2022)

[14] Eglen, R.M.: Functional g protein-coupled receptor assays for primary and secondary screening. Combinatorial chemistry & high throughput screening **8**(4), 311–318 (2005)

[15] Eiger, D.S., Pham, U., Gardner, J., Hicks, C., Rajagopal, S.: Gpcr systems pharmacology: a different perspective on the development of biased therapeutics. American Journal of Physiology-Cell Physiology **322**(5), C887–C895 (2022)

[16] Feynman, R.P.: Statistical mechanics: a set of lectures. CRC press (2018)

[17] Filipek, S.: Molecular switches in gpcrs. Current opinion in structural biology **55**, 114–120 (2019)

[18] Forestiero, S.: The historical nature of biological complexity and the ineffectiveness of the mathematical approach to it. Theory in Biosciences **141**(2), 213–231 (2022)

[19] Franco, R., Rivas-Santisteban, R., Reyes-Resina, I., Navarro, G.: The old and new visions of biased agonism through the prism of adenosine receptor signaling and receptor/receptor and receptor/protein interactions. Frontiers in Pharmacology **11**, 628601 (2021)

[20] Frigg, R., Werndl, C.: Entropy-a guide for the perplexed (2011)

[21] Gerstein, M., Echols, N.: Exploring the range of protein flexibility, from a structural proteomics perspective. Current opinion in chemical biology **8**(1), 14–19 (2004)

[22] Ginsburg, G.S., Phillips, K.A.: Precision medicine: from science to value. Health Affairs **37**(5), 694–701 (2018), doi: 10.1377/hlthaff.2017.1624. PMID: 29733705; PMCID: PMC5989714.

[23] Grover, J.: A literature review of bayes' theorem and bayesian belief networks (bbn). Strategic economic decision-making: using Bayesian belief networks to solve complex problems pp. 11–27 (2012)

[24] Haseltine, W.A., Patarca, R.: The rna revolution in the central molecular biology dogma evolution. International Journal of Molecular Sciences **25**(23), 12695 (2024)

[25] Hébert-Dufresne, L., Allard, A., Garland, J., Hobson, E.A., Zaman, L.: The path of complexity. npj Complexity **1**(1), 4 (2024)

[26] Homans, S.W.: Water, water everywhere—except where it matters? Drug discovery today **12**(13-14), 534–539 (2007)

[27] Ireson, G.: Einstein and the nature of thought experiments. School Science Review **86**(317), 47–53 (2005)

[28] Jacobs, D.J., Rader, A.J., Kuhn, L.A., Thorpe, M.F.: Protein flexibility predictions using graph theory. Proteins: Structure, Function, and Bioinformatics **44**(2), 150–165 (2001)

[29] Jones, A.M.: Vps26 moonlights as an arrestin-like adapter for a 7-transmembrane rgs 2 protein in arabidopsis thaliana. Tech. rep., University of North Carolina, Chapel Hill, NC (United States) (2023)

[30] Jones, R.D.: Information transmission in g protein-coupled receptors. International Journal of Molecular Sciences **25**(3), 1621 (2024)

[31] Jones, R.D., Jones, A.M.: Model of ligand-triggered information transmission in g-protein coupled receptor complexes. Frontiers in Endocrinology **14**, 879 (2023)

[32] Jones, R.D., Jones, A.M.: A proposed mechanism for in vivo programming transmembrane receptors. In: Italian Workshop on Artificial Life and Evolutionary Computation. pp. 123–137. Springer (2023)

[33] Kaila, V.R., Annila, A.: Natural selection for least action. Proceedings of the Royal Society A: Mathematical, Physical and Engineering Sciences **464**(2099), 3055–3070 (2008)

[34] Karshikoff, A., Nilsson, L., Ladenstein, R.: Rigidity versus flexibility: the dilemma of understanding protein thermal stability. The FEBS journal **282**(20), 3899–3917 (2015)

[35] Keshelava, A., Solis, G.P., Hersch, M., Koval, A., Kryuchkov, M., Bergmann, S., Katanaev, V.L.: High capacity in g protein-coupled receptor signaling. Nature communications **9**(1), 1–8 (2018)

[36] Kise, R., Inoue, A.: Gpcr signaling bias: an emerging framework for opioid drug development. The Journal of Biochemistry p. mvae013 (2024)

[37] Koenig, I.R., Fuchs, O., Hansen, G., von Mutius, E., Kopp, M.V.: What is precision medicine? European respiratory journal **50**(4) (2017), doi: 10.1183/13993003.00391-2017. PMID: 29051268.

[38] Kolb, P., Kenakin, T., Alexander, S.P., Bermudez, M., Bohn, L.M., Breinholt, C.S., Bouvier, M., Hill, S.J., Kostenis, E., Martemyanov, K.A., et al.: Community guidelines for gpcr ligand bias: Iuphar review 32. British journal of pharmacology **179**(14), 3651–3674 (2022)

[39] Kosorok, M.R., Laber, E.B.: Precision medicine. Annual review of statistics and its application **6**, 263–286 (2019), doi: 10.1146/annurev-statistics-030718-105251. PMID: 31073534; PMCID: PMC6502478.

[40] Landauer, R.: The physical nature of information. Physics letters A **217**(4-5), 188–193 (1996)

[41] Latorraca, N.R., Masureel, M., Hollingsworth, S.A., Heydenreich, F.M., Suomivuori, C.M., Brinton, C., Townshend, R.J., Bouvier, M., Kobilka, B.K., Dror, R.O.: How gpcr phosphorylation patterns orchestrate arrestin-mediated signaling. Cell **183**(7), 1813–1825 (2020)

[42] Latorraca, N.R., Wang, J.K., Bauer, B., Townshend, R.J., Hollingsworth, S.A., Olivieri, J.E., Xu, H.E., Sommer, M.E., Dror, R.O.: Molecular mechanism of gpcr-mediated arrestin activation. Nature **557**(7705), 452–456 (2018)

[43] Leighton, M.P., Sivak, D.A.: Flow of energy and information in molecular machines. Annual Review of Physical Chemistry **76** (2025)

[44] Lundstrom, K.: Present and future approaches to screening of g-protein-coupled receptors. Future Medicinal Chemistry **5**(5), 523–538 (2013)

[45] Mahoney, J.P., Sunahara, R.K.: Mechanistic insights into GPCR–G protein interactions. Current opinion in structural biology **41**, 247–254 (2016)

[46] Marsh, J.A., Teichmann, S.A., Forman-Kay, J.D.: Probing the diverse landscape of protein flexibility and binding. Current opinion in structural biology **22**(5), 643–650 (2012)

[47] Miller Jr, W.B., Baluška, F., Reber, A.S., Slijepčević, P.: Biology in the 21st century: Natural selection is cognitive selection. Progress in Biophysics and Molecular Biology **190**, 170–184 (2024)

[48] Morowitz, H., Smith, E.: Energy flow and the organization of life. Complexity **13**(1), 51–59 (2007)

[49] Palmer, S.J.: The thermodynamic forces driving natural selection and their evolutionary consequences. The Journal of Physical Chemistry **17** (2018)

[50] Phillips, R.: Schrödinger's what is life? at 75. Cell systems **12**(6), 465–476 (2021)

[51] Prigogine, I.: Time, structure, and fluctuations. Science **201**(4358), 777–785 (1978)

[52] Qian, H.: Phosphorylation energy hypothesis: open chemical systems and their biological functions. Annu. Rev. Phys. Chem. **58**, 113–142 (2007)

[53] Reif, F.: Fundamentals of statistical and thermal physics. Waveland Press (2009)

[54] Rosing, J., Slater, E.: The value of δg° for the hydrolysis of atp. Biochimica et Biophysica Acta (BBA)-Bioenergetics **267**(2), 275–290 (1972)

[55] Santos, R., Ursu, O., Gaulton, A., Bento, A.P., Donadi, R.S., Bologa, C.G., Karlsson, A., Al-Lazikani, B., Hersey, A., Oprea, T.I., et al.: A comprehensive map of molecular drug targets. Nature reviews Drug discovery **16**(1), 19–34 (2017)

[56] Sauer, M.F., Sevy, A.M., Crowe Jr, J.E., Meiler, J.: Multi-state design of flexible proteins predicts sequences optimal for conformational change. PLoS computational biology **16**(2), e1007339 (2020)

[57] Schlessinger, J.: Cell signaling by receptor tyrosine kinases. Cell **103**(2), 211–225 (2000)

[58] Schrodinger, R., Schrödinger, E., Dinger, E.S.: What is life?: With mind and matter and autobiographical sketches. Cambridge university press (1992)

[59] Shannon, C., Weaver, W.: The mathematical theory of communication,(first published in 1949). Urbana University of Illinois Press (1963)

[60] Sivasankar, V.S., Zia, R.N.: The matter/life nexus in biological cells. Annual Review of Chemical and Biomolecular Engineering **16**(1), 409–432 (2025)

[61] Skiba, M., Stolwijk, J.A., Wegener, J.: Label-free impedance measurements to unravel biomolecular interactions involved in g protein-coupled receptor signaling. In: Methods in Cell Biology, vol. 169, pp. 221–236. Elsevier (2022)

[62] Stolwijk, J.A., Skiba, M., Kade, C., Bernhardt, G., Buschauer, A., Hübner, H., Gmeiner, P., Wegener, J.: Increasing the throughput of

label-free cell assays to study the activation of g-protein-coupled receptors by using a serial agonist exposure protocol. Integrative Biology **11**(3), 99–108 (2019)

[63] Teilum, K., Olsen, J.G., Kragelund, B.B.: Functional aspects of protein flexibility. Cellular and Molecular Life Sciences **66**(14), 2231–2247 (2009)

[64] Teilum, K., Olsen, J.G., Kragelund, B.B.: Protein stability, flexibility and function. Biochimica et Biophysica Acta (BBA)-Proteins and Proteomics **1814**(8), 969–976 (2011)

[65] Wackerhage, H., Hoffmann, U., Essfeld, D., Leyk, D., Mueller, K., Zange, J.: Recovery of free adp, pi, and free energy of atp hydrolysis in human skeletal muscle. Journal of applied physiology **85**(6), 2140–2145 (1998)

[66] Wegener, J., Zink, S., Rösen, P., Galla, H.J.: Use of electrochemical impedance measurements to monitor β-adrenergic stimulation of bovine aortic endothelial cells. Pflügers Archiv **437**, 925–934 (1999)

[67] William B. Miller, J., Cárdenas-García, J.F., Reber, F.B.A.S., Slijepčević, P., Little, J.C.: BioSystems (in Press)

[68] Wirth, U., Erl, J., Azzam, S., Höring, C., Skiba, M., Singh, R., Hochmuth, K., Keller, M., Wegener, J., König, B.: Monitoring the reversibility of gpcr signaling by combining photochromic ligands with label-free impedance analysis. Angewandte Chemie **135**(21), e202215547 (2023)

[69] Yang, Z., Yang, F., Zhang, D., Liu, Z., Lin, A., Liu, C., Xiao, P., Yu, X., Sun, J.P.: Phosphorylation of g protein-coupled receptors: from the barcode hypothesis to the flute model. Molecular pharmacology **92**(3), 201–210 (2017)

[70] Zhang, M., Chen, T., Lu, X., Lan, X., Chen, Z., Lu, S.: G protein-coupled receptors (gpcrs): advances in structures, mechanisms and drug discovery. Signal transduction and targeted therapy **9**(1), 88 (2024)

Appendix A. Theory

Appendix A.1. Information and the Second Law of Thermodynamics

Standard equilibrium techniques that analyze systems by minimizing free energy do not apply to information-processing systems. Because information processing requires continuous energy and entropy flow, even in steady state [40], entropy maximization is not achievable in non-isolated systems [INSERT REFERENCE TO WIVACE PAPER].

The entropy S of a system composed of W states x_i is

$$S = -\sum_{i=1}^{W} \Pr(x_i) \ln \Pr(x_i) \tag{A.1}$$

Assume that the system is composed of a switch in the form of a chemical reaction

$$\mathrm{u} \rightleftharpoons \mathrm{b} \tag{A.2}$$

where, as an example, d is the dephosphorylated state of the switch and p is the phosphorylated state of the switch. The rest of the system is a heat bath that absorbs heat that is generated by the chemical reaction. The entropy, Eq. A.1, can then be written

$$S = S_m - I_M \tag{A.3}$$

where S_m is the entropy of the microstates given that the observables d and p is the switch are independent and I_M is the information in the correlation of the mesoscopic components d and p of the switch. The microscopic entropy S_m is composed of two pieces, the entropy of the microscopic components of the switch and the microscopic entropy of the microstates of the external heat bath. The entropy of the microstates is

$$S_m = \sum_{i=1}^{W} \Pr(x_i, d, p) \ln \left[\frac{\Pr(d, p)}{\Pr(x_i) \Pr(d) \Pr(p)} \right] \tag{A.4}$$

where $\Pr(d, p)$ is the joint probability of d and p.

The mutual information [59] associated with the correlation of d and p is

$$I_M = \sum_{\{d,p\}} \Pr(d, p) \ln \left[\frac{\Pr(d, p)}{\Pr(d) \Pr(p)} \right] \tag{A.5}$$

The Second Law of Thermodynamics states that the entropy of the system increases with time or achieves a maximum value.

$$\Delta S = \Delta S_m - \Delta I_M \geq 0 \tag{A.6}$$

If the number of states W is infinite, the system never achieves a maximum value.

In the case that the switch achieves a steady state $\Delta I_S \to 0$, then all the entropy generated by the switch goes into the heat bath.

$$\Delta S \to \Delta S_m \geq 0 \tag{A.7}$$

When the switch has reached steady state $\Delta I_M \to 0$, the switch information I_M is at an extremum.

For a system with an infinite number of states W, total entropy continues to increase indefinitely. Local regions of correlation, such as molecular switches, can achieve steady states even as the entropy of the larger system grows. The heat generated by the switch is transferred to the surrounding heat bath. This scenario contrasts with finite systems W, where the total entropy S can reach a maximum. Because biological information processing systems function far from equilibrium, traditional frameworks based on minimizing Gibbs free energy $G = E - TS$, with E as the energy of the system and T the temperature of the bath do not apply.

Appendix A.2. Theoretical Model of the Switch

Building on our earlier theoretical framework [31, 32, 30], which successfully predicted the results of the experimental assay by maximizing the flow of information from the extracellular environment to the intracellular region of the GPCR complex, the present work extends this theory by incorporating a higher temporal resolution. This enhanced model is specifically developed to interpret the detailed, time-dependent dynamics observed in recent impedance-based experiments by Wirth et al. [68]. In line with its predecessor, this updated model is guided by the fundamental principle that natural selection favors molecular systems optimized to maximize information transmission capacity [59], thus providing a more granular and dynamic view of the GPCR switching mechanisms.

Figures 2B and 2C presents a simplified mathematical representation of the schematic shown in Figure 2A. This abstraction allows for a more tractable analysis using the tools of statistical mechanics [53]. This level of

simplification is common and has been useful in physics [12, 27]. In this model, the GPCR complex is reduced to a single switch embedded in a heat bath and surrounded by a flexible protein matrix [34, 21, 46, 28, 56, 7, 64, 63, 26]. The probabilities $\Pr(d)$ and $\Pr(p)$ represent the fraction of time the receptor spends in the dephosphorylated and phosphorylated states, respectively. Specifically, the d position corresponds to the state in which the G protein is bound to a GDP molecule, while the p position corresponds to the state in which GDP has been phosphorylated to form GTP. During a time interval Δt, the switch can transition between these states with transition probabilities $\Pr(d|p)$ and $\Pr(p|d)$, or it can remain in the same state with probabilities $\Pr(u|u)$ and $\Pr(b|b)$. The heat bath ensures that the fluctuations between these switching states occur as if the system is at a temperature $T = 1/\beta$, where T is in energy units.

Figure 2C describes the switch in terms of chemical flux

$$J_0 = \Pr(p|d)\ \Pr(d) = \Pr(d|p)\ \Pr(p) \tag{A.8}$$

which represents the flow of probability from one switch position to another. This description is useful if the switch is fueled by an external source such as a GTP/GDP disequilibrium. A flow of energy from GTP/GDP into the switch is turned into heat $Q_\odot$ in the time interval Δt

$$Q_\odot = J_0\ q = -\Delta G_\odot \tag{A.9}$$

where $-q$ is the amount of heat released when a GPCR transitions from the "off" position to the "on" position and back; and ΔG is the amount of the free energy from GTP that is injected into the switch in time Δt. The minus sign indicates that the heat is leaving the switch. Equation A.9 describes the flow of entropy through the switch. A flow of entropy of this nature is essential for life [48]. We take flux J_0 as the external driver of emergent behavior in the switching system.

The details of ligand/receptor binding are an important part of the overall picture. The inclusion of ligand kinetics is shown in Figure 2D. The interaction between the ligand and the free receptor f to form the bound associated state a is modeled using Michaelis-Menten kinetics [6]. The forward reaction rate is given by k_+L where L represents the ligand concentration, while the reverse reaction rate is k_-

Within the associated state a, the receptor can adopt different internal states corresponding to the switch positions. The probability that the receptor is in the dephosphorylated "off-"state d given that it is in a is denoted as

$\Pr(u|a)$. Similarly, the probability that the receptor is in the phosphorylated "on" state is $\Pr(b|a)$. The observed probabilities $\Pr(d)$ and $\Pr(p)$ are

$$\Pr(d) = \Pr(a)\ \Pr(u|a) \tag{A.10}$$

and

$$\Pr(p) = \Pr(a)\ \Pr(b|a) \tag{A.11}$$

Aspects of the ligand/receptor binding kinetics were observed in [68]. Specifically, it was observed that the ligands remained bound to within the time range of the experiment even if the extracellular fluid was washed free of ligands. The details of these observations provide insight into the role that the switch position plays in ligand binding. In this study, we do not address this process. This will be addressed in a follow-up study.

The transmission of information I [59, 2, 20] through the switch is:

$$I = \sum_{i\in\{d,p\}} \sum_{j\in\{d,p\}} \Pr(j|i)\ \Pr(i)\ \log\left(\frac{\Pr(i|j)}{\Pr(i)}\right) \tag{A.12}$$

$$I = J_0 \log\left(\frac{\Pr(d|p)\ \Pr(p|d)}{\Pr(d)\ \Pr(p)}\right) + (\Pr(d) - J_0)\log\left(\frac{\Pr(u|u)}{\Pr(d)}\right) + (\Pr(p) - J_0)\log\left(\frac{\Pr(b|b)}{\Pr(p)}\right) \tag{A.13}$$

Maximization of the information transmitted through the switch subject to the constraints that the total energy $\bar{E}$ of the switch is given and the flux J_0 is an externally determined constant leads to what we refer to as the Biological Ensemble

$$\Pr(d)^2\ [\ \Pr(p) - J_0\ ]\ \exp(-\beta E_p)\ =\ \Pr(p)^2\ [\ \Pr(d) - J_0\ ]\exp(-\beta E_d) \tag{A.14}$$

$$\bar{E} = \Pr(d)\ E_d + \Pr(p)\ E_p \tag{A.15}$$

where E_d is the energy of the switch in the off position and E_p is the energy of the switch in the on position. The word "ensemble" is commonly used in two related concepts. It can be used to describe the probability given by Eq. A.14 of finding a switch in the p position or it can describe an imaginary collection of switch states that have probability given by Eq. A.14 or another equation such as the Canonical Ensemble [53].

The Biological Ensemble, Eq. A.14, determines the theoretical outcomes and testable predictions that can be used to inform the experimental observations of [68]. Like the Canonical Ensemble in equilibrium thermodynamics [53], the Biological Ensemble can predict microscopically observable behavior such as the impedance measurements described in the previous section. To see this, we assumed that the switch positions are correlated with the GPCR conformations generated by the Z and E forms of the ligand. It follows that Eq. A.14 predicts the relationships among the impedance observations in [68]

Three solutions of the biological ensemble exist for small chemical flux $J_0 = 0$ (Figure 3A). One solution (yellow) corresponds to the Canonical Ensemble [53] valid for systems in thermal equilibrium. We refer to this solution for all permissible flux values J_0 as the Thermodynamic Branch [51]. Two other solutions are $\Pr(p) = 1,\ \Pr(d) = 1 - \Pr(p) = 0$ and $\Pr(p) = 0,\ \Pr(d) = 1 - \Pr(p) = 1$ (blue and red). We refer to these solutions as the kinetic branch. It should be noted that $J_0 = 0$ represents the conditions typically used to determine ligand binding to receptor equilibrium constants (binding isotherms) and rate constants (dissociation rate).

The solutions in Figure 3 represent the local maximums of information transmission. The capacity of the system is at a local maximum in the solutions. Two parameters determine the system output, the change in free energy $\beta(E_p - E_d)$ and the externally driven flux J_0. Rapid shifts in these two quantities may initiate a shift from one local maximum to another.

For most pharmaceutical applications, the control parameters are altered by changes in the ligand and ligand conformation. Of particular importance are jumps initiated by a change in ligand or ligand conformation that move the switch from the "on position, $\Pr(p) \to 1$ to the "off position, $\Pr(d) = 1 - \Pr(p) \to 1$. One type of jump among solutions is particularly important, jumps in which changes in ligand conformation lead to changes in the switch position. This permits the ligand, which may be a drug, to control the downstream cellular response to the ligand. In this study, we focus on the identification of these jumps in the observations in [68]. This informs the efficacy of a drug candidate.

Appendix B. Connection Between Experiment and Theory

The experimenters in [68] assumed the existence of a strong correlation between the measured impedance and the downstream response. We explic-

itly assume the simplest relationship between impedance and response, which is linear

$$\Pr(d) = 1 - \Pr(p) = \frac{Z - Z_{DMSO}}{Z_{hPP} - Z_{DMSO}}, \tag{B.1}$$

where Z_{hPP} is the impedance measured with the endogenous agonist human pancreatic polypeptide (hPP) and Z_{DMSO} is the impedance for the solvent DMSO (negative control). The Biological Ensemble is symmetric upon interchange of p and d. Therefore, Eq. B.1 with p replaced with d is also a possible connection between experiment and theory. As long as the relationship between $\Pr(p)$ and Z is monotonic, the conclusions of this paper should not be affected by the exact form of Eq. B.1. hPP and DMSO were used to define the boundaries of observable impedance in [68]. The connection between impedance Z and probability of the "on" position $\Pr(d)$ provides visibility into how flux J_0 and change in free energy $\beta(E_p - E_d)$ change in response to various ligand molecules and conformations of the molecules. Figure 3 provides the map for the relationship between impedance and control parameters J_0 and change in free energy for each ligand.

Appendix C. Information Landscape

Figure C.7 presents a conceptual schematic of the information landscape described in Section 3.2, with the two control parameters, $\beta(E_p - E_d)$ and J_0, plotted along the horizontal axes and the information content of the system on the vertical axis. The surface contains peaks and valleys, representing points where the time derivative of the information content is zero. These extrema correspond to the NESS of the system. The specific NESS for the modeled system are mapped in Figure 3. Each ridge in Figure C.7 marks a local information maximum, although not necessarily the global maximum.

In Figure C.8, the global maxima of the Biological Ensemble solutions are shown in black. Within this model, these black trajectories correspond to the highest possible information transmission and thus represent the most probable states of the system. The remaining trajectories represent local maxima, quasistable states that can persist for extended periods, but are less likely to occur naturally. For a system residing in one of these local maxima to transition to the global maximum, it must experience a sufficiently large perturbation to overcome the stability of the local state.

At the critical flux

$$J_0 = \phi_c \approx 0.182 \tag{C.1}$$

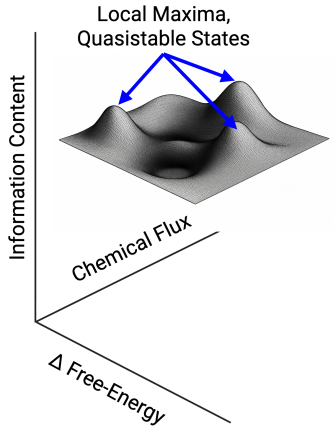

Figure C.7: The two control parameters are given by the change in the free energy of phosphate bonding, $\beta(E_p - E_d)$, and the chemical flux, J_0. The information content of the system is displayed on the vertical axis. Local maxima and minima of the information are locations of steady state for information content of the system.

The maximum information in the thermodynamic branch and the kinetic branch is equal at free energy $\beta(E_p - E_d)$ For flux greater than ϕ_c two small isolated solution islands appear as seen in Figures C.8D-G. As the flux J_0 increases further, the regimes eventually merge into a single continuous solution at the maximum information value of $J_0 = 1/2$, as seen in Figure C.8I.

Figures C.8 B-I illustrate the three solutions as the flux J_0 increases. At

$$J_0 = \frac{1}{4} \tag{C.2}$$

the thermodynamic branch reduces to the "off" state $Pr(p) = 0$ leaving only the kinetic branch with finite probability for $Pr(p)$. The thermodynamic branch contains zero entropy and information for $J_0 > 1/4$. Figs. 3G-I illustrate the supercritical behavior of the two solutions of the kinetic branch in this regime.

It is important to note that the optimal maximum-information solution for the NESS is discontinuous. Phase transitions occur within the phase

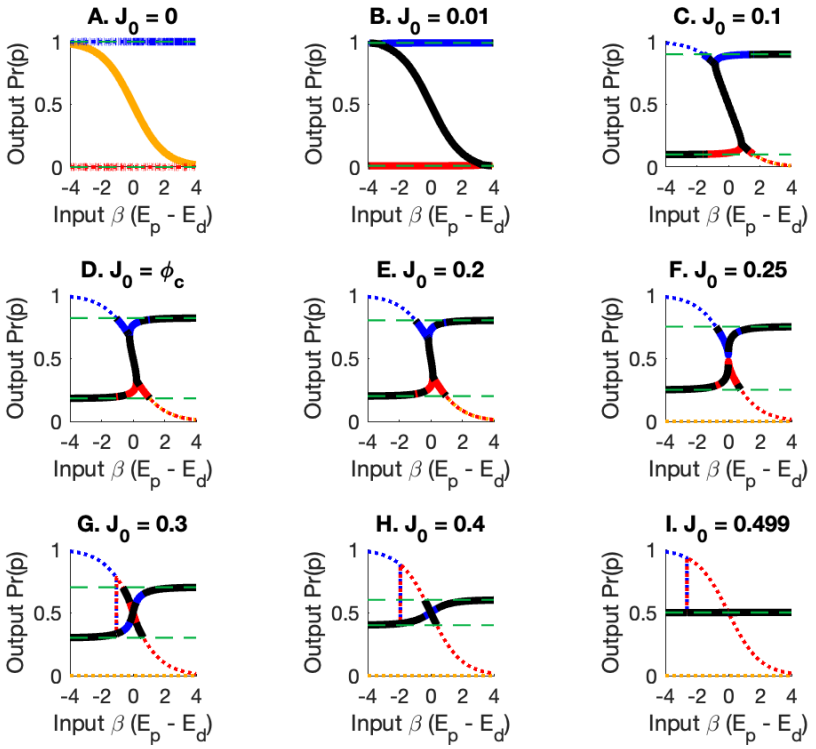

Figure C.8: The paths with the largest information transmission are outlined in black. **A.** In the limit of zero flux, all paths have the same information transmission. **B.** For a very small but finite flux J_0, the thermodynamic branch has the highest capacity. The highest capacity path for probability $Pr(p)$ obeys the Canonical Ensemble. **B.-I.** For a given flux J_0, discontinuities in the high capacity path appear with changes in binding energy $\beta(E_p - E_d)$ The highest-capacity path represents a global maximum, while the other possible paths represent local maximum, or quasi-stable states of the switch.

space defined by the control parameters J_0 and $\beta(E_p - E_d)$. This implies that for a given flux J_0, a minor change in the binding energy can lead to a significant alteration in the switch state - "on" or "off", particularly when the energy is adjusted near a phase transition. Moreover, the system can be prepared to lie on paths of local maximum of capacity. These states can transition to the global maximum with a sufficient perturbation.